frontiers | Frontiers in Marine Science

TYPE Original Research
PUBLISHED 24 November 2022
DOI 10.3389/fmars.2022.1074829

OPEN ACCESS

EDITED BY
Wen Zhuang,
Shandong University, China

REVIEWED BY
Kai Liu,
Dongying Research Institute for Oceanography Development, China
Fan Zhang,
Yunnan University of Traditional Chinese Medicine, China
Yuxuan Zhang,
Chinese Research Academy of Environmental Sciences, China

*CORRESPONDENCE
Yuxi Lu
yxlu@yic.ac.cn
Ning Wang
nwang@yic.ac.cn

SPECIALTY SECTION
This article was submitted to Marine Biogeochemistry, a section of the journal Frontiers in Marine Science

RECEIVED 20 October 2022
ACCEPTED 10 November 2022
PUBLISHED 24 November 2022

CITATION
Luan F, Yang T, Lu Y and Wang N (2022) Molecular size-fraction and seasonal characteristics of dissolved trace metals in river and estuarine waters of the Yellow River, China. *Front. Mar. Sci.* 9:1074829. doi: 10.3389/fmars.2022.1074829

Molecular size-fraction and seasonal characteristics of dissolved trace metals in river and estuarine waters of the Yellow River, China

Feng Luan[1], Tingting Yang[1], Yuxi Lu[2,3]* and Ning Wang[2,3]*

[1]College of Chemistry and Chemical Engineering, Yantai University, Yantai, China, [2]CAS Key Laboratory of Coastal Environmental Processes and Ecological Remediation, Research Center for Coastal Environment Engineering Technology of Shandong Province, Yantai Institute of Coastal Zone Research, Chinese Academy of Sciences, Yantai, China, [3]Shandong Key Laboratory of Coastal Environmental Processes, Yantai, China

The colloidal phase is an important metal storage form in the aquatic system. However, its biogeochemical behavior in the estuarine environment has been seldom studied. In this study, spatial variations, sources and correlations with seawater environmental factors of the dissolved Fe, Mn, Cu, Zn, Cd and Pb in the surface water of the Yellow River Estuary in China were investigated. The clean sampling system, centrifugal ultrafiltration technique, and ICP-MS were combined and used for the determination of the colloidal distribution of six metals in this region. Two stations of Zn in autumn had contamination factor values >1, which indicates lower contaminant levels of Cu, Zn, Cd and Pb. Dissolved target metal was divided into five fractions, i.e. <1 kDa, 1-3 kDa, 3-10 kDa, 10-100 kDa and 100 kDa-0.45 μm, while the average concentrations of each fraction were 60.17, 46.54, 47.73, 251.03, 1.44 and 1.08 nmol L^{-1} in spring and 62.30, 48.18, 15.35, 203.05, 1.20 and 1.70 nmol L^{-1} in autumn, respectively. The results showed that colloidal Mn, Cu, Zn, Cd and Pb might be dominated by high-molecular-weight fraction (100 kDa-0.45 μm). Additionally, the contribution of low-molecular-weight colloidal Fe (1-10 kDa) in this aquatic system was obvious. The addition in the colloidal and total dissolved fraction might be mainly related to particle-desorbed ligand, which was usually occurred in the middle salinity area. Dissolved organic carbon (DOC) and colloidal organic carbon (COC) concentration could not correlate with the behavior of Mn, Zn and Cd, which proved that the influence of inorganic ligands was higher than that of organic ligands or biological contributions, but the influence of salinity, dissolved oxygen (DO), pH and temperature should not be ignored. Overall, the results suggested that the occurrence of dynamic behaviors of colloidal metal in the YRE was highly associated with the salinity transition and formation of the organic matter-particle mixture system under complex hydrodynamic processes.

KEYWORDS

Yellow River Estuary, colloidal trace metal, centrifugal ultrafiltration, molecular size-fraction, geochemical feature

1 Introduction

The studies of the basic morphology of metals in the aquatic system are usually carried out by filtration through a 0.2 μm, 0.45 μm or 1 μm pore size filter, and the trace elements are simply divided into two parts, i.e. dissolved and particulate phases (Zhou et al., 2016; Lu et al., 2022). However, the part considered to be dissolved contains many colloidal particles that are easily overlooked, and it plays a significant biogeochemical role in the aquatic environment (Guo and Santschi, 2007; Xu et al., 2018a; Xu et al., 2018b; Xu et al., 2018c). In recent years, with the application of cross-flow ultrafiltration, centrifugal ultrafiltration (CFU) and other technologies, the research on the determination of colloidal trace elements in aquatic systems has been developed rapidly (Liu et al., 2013; Lu et al., 2019). Similarly, these studies found that most of the dissolved metals exist in the form of small-sized inorganic particles or macromolecular organic matter (ie, colloidal phase) in the aquatic environment, which largely participates in the operation of the water environment ecosystem (Cornu et al., 2018). For example, as the common and essential metal micronutrients, Fe, Cu and Zn play a significant role in plant metabolism by participating in electron transport, nitrate reduction, photosynthesis, respiration, chlorophyll synthesis, and so on (Han et al., 2021). Among them, Cu plays an important role in marine ecosystems (Peers and Price, 2006). For example, most phytoplankton requires Cu to perform some key redox effects, which has attracted more and more attention to its research (Illuminati et al., 2017; González-Álvarez et al., 2020). As an important biologically active metal, Cu has been proved in many studies to be easily adsorbed on inorganic/organic ligands in the water environment, thereby increasing its bioavailability, and maybe the important environmental factor for causing red tides, green tides and algal blooms in the nearshore area (Lu et al., 2021). Typical toxic heavy metals such as Cd and Pb may accumulate along the food chain, thereby threatening aquatic organisms and human health (Lu et al., 2019; Liang et al., 2022). Therefore, the study of the morphology of trace metals, especially the colloidal phase, is of great significance for understanding the morphological distribution and geochemical behavior of metals in the aquatic systems (Wen et al., 2011; Statham et al., 2012; Lu et al., 2020).

The Yellow River is the second-longest river in China with a basin area of ~ 7915 km^2 (Wang et al., 2016). It runs through northern China and brings a large number of pollutants from urban, agriculture and industrial pollutants into the Bohai Sea (Tang et al., 2010). The Yellow River Estuary (YRE) is an important fishing area in China and provides spawning sites for many aquatic organisms in the Bohai Sea and the Yellow Sea (Liu et al., 2018). In addition, it is adjacent to Shengli Oilfield (the second-largest oilfield of China) and the Yellow River Delta National Nature Reserve (Wang et al., 2011). The Yellow River flows through the world's largest loess deposit area, the Loess Plateau in north-central China, and carries a large number of suspended particulate matter (SPM) and freshwater, making it register as the world's most turbid river and the dominant land-based factor in the Bohai Sea (Zhang and Huang, 1993; Milliman and Ren, 1995; Bi et al., 2014). Therefore, great concern has been attracted in this area due to its unique environmental significance, ecological sensitivity and environmental conditions (Liu et al., 2016a and Liu et al., 2016b; Wang et al., 2018; Lu et al., 2021).

Previous studies of the YRE focused on the concentration, distribution, and environmental impact of trace elements in water and particulate matter (Qiao et al., 2007; Tang et al., 2010; Lin et al., 2016; Wang et al., 2018). However, minimal researches are available about the fate, migration and environmental behavior of the trace elements in this region, especially colloidal phases. Therefore, the dissolved metals in the YRE surface water were investigated through two sampling surveys in March and November 2021. The major objectives of our present research work were to: (1) introduce a self-made clean sampling technique and a fully enclosed pre-filtration system; (2) study the abundance and compositional variations of Fe, Mn, Cu, Zn, Cd and Pb in five molecular weight size ranges of dissolved phase in the river-sea mixing area; (3) reveal the specific molecular weight (MW) colloids that can regulate the behavior of colloidal Fe, Mn, Cu, Zn, Cd and Pb environmental conditions in this region; (4) explore the relationship between the dynamic behavior of target element and environmental factors in the five fraction of the dissolved phase. The basis for selecting these five dissolved fractions is that they cover the truly dissolved phase (<1 kDa), the low-molecular-weight (LMW) colloidal phase and the high-molecular-weight (HMW) colloidal phase, so as to facilitate the subsequent detailed evaluation of metal migration between each fraction. The results are the original report of colloidal Fe, Mn, Cu, Zn, Cd and Pb of the YRE and can provide some new insights into the geochemical feature and heterogeneity of micronutrient elements in the river-sea continuum and the aquatic system.

2 Material and methods

2.1 Sampling and pre-filtration

The internal-fluorinated high-density polyethylene (HDPE) bottles for sampling were pre-cleaned using a method reported by Lu et al. (2020 and Lu et al., 2021). Briefly, after being rinsed with Decon 90™ detergent (10%, v/v) 3 times, each bottle was stored in 1.5 M nitric acid (HNO_3) and 1.2 M hydrochloric acid (HCl) for 48 h, respectively, and finally rinsed with ultra-pure water (R = 18.2 MΩ-cm) which was produced by a Purelab Classic water purification system (ELGA Labwater, UK). The

HNO_3 and HCl used in the experiment were prepared by diluting high concentration, purchased from the Sinopharm Chemical Reagent Co., Ltd., China and processed by the sub-boiling distillation equipment before use. All labware in contact with samples or sub-samples must also be pre-cleaned using the above method and dried in a clean bench, and then double-packed until sampling.

The samples and field data used in this study were obtained through two cruises which were conducted in March (spring flood at peach-blossom time) and November (autumn, dry season of the Yellow River) 2021. 1 L of the surface water samples (1 m deep) were collected manually on a boat from 9 sites (Figure 1). The standard of water depth in this study referred to the study of Yang et al. (2020). The main body of the home-made pole-sampling equipment was equipped with a Teflon rod main body and the internal-fluorinated HDPE bottle was bound with disposable Nylon cable ties. The salinity, dissolved oxygen (DO), temperature and pH of the samples were measured by using the portable multi-parameter water quality analyzer (YSI ProPlus, USA). After the water sample was collected, put the sampling bottle in a polyethylene bag immediately and store it in a cooler box at about 4°C. After returning to the laboratory, the samples were pre-filtered immediately using a homemade fully enclosed filtration system. The system consists of a peristaltic pump, a diaphragm vacuum pump, pipes and a filter cover. The main working principle was as follows: first, unfiltered water samples were pumped along the C-flex® tubing into the upper part of the polysulfone vacuum filtration device by using a Masterflex® L/S peristaltic pump; secondly, the vacuum pump was turned on to perform fully enclosed real-time filtration of the sample; finally, the filtered water samples could be collected in another pre-cleaned HDPE bottles for further processing. The storage method of filtered samples was the same as that of unfiltered samples.

2.2 Centrifugal ultrafiltration

Four kinds of Macrosep® centrifugal ultrafiltration units (Pall Laboratory) with respective molecular weight cutoffs (MWCOs) of 1, 3, 10 and 100 kDa (Model: MAP010C38) were used with a Velocity 14R centrifuge (Dynamica Corporation, Australia). Before ultrafiltration, each unit was sequentially washed with 10 mL 0.05 M NaOH, 10 mL 0.02 M HCl and 10 mL ultra-pure water for 5-10 times to remove possible background (Lu et al., 2020). Each unit was then loaded with 15 mL of <0.45 μm pre-filtered samples, and centrifuged (4°C, 4200 × g, 50-70 min) to ≤0.5 mL to separate the ultrafiltrate (<1 kDa, <3 kDa, <10 kDa and <100 kDa) for the characterization of colloids with different molecular weight sizes (Lu et al., 2020). After CFU, 0.2 mL ultrafiltrate was pipetted and diluted to 10 mL with 0.5 M HNO_3. <0.45 μm total dissolved (TD) phase was treated in the same process. As for the concentrate, 3 mL 0.5 M HNO_3 was added in parallel for extracting metals. Then, 3 parallel extracts were well mixed and volume adjusted to 5 mL with 0.5 M HNO_3. All sub-samples were stable at room temperature (~25°C) for ≥48 h and then measured using an inductively coupled plasma mass spectrometer (ICP-MS). According to the concentration difference between the initial filtered sub-samples and the ultrafiltrate, the concentrations of colloidal metals in different size ranges were calculated (Lu et al., 2020). Finally, size fractions of colloidal metal can be defined as 1-3 kDa, 3-10 kDa, 10-100 kDa and 100 kDa-0.45 μm, and <1 kDa fraction was defined as the truly dissolved phase.

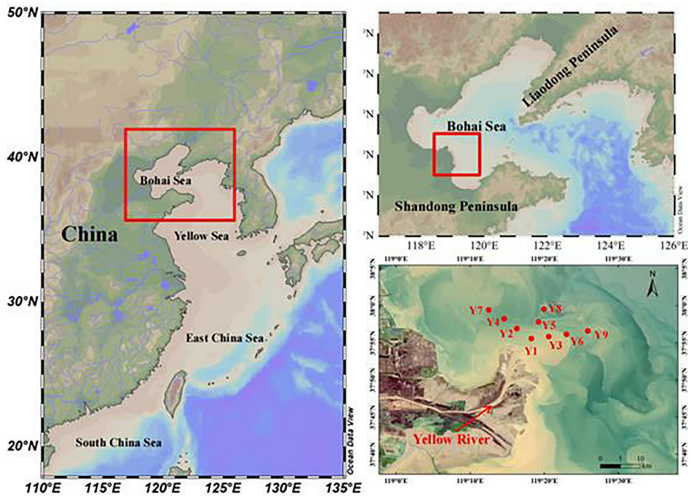

FIGURE 1
Location of sampling sites in the study area.

2.3 Analytical methods

2.3.1 Metal determination

For the water samples, metals in prefiltered waters, ultrafiltrate and concentrate were acid-extracted (using 0.5 M HNO_3) and directly determined by ELAN DRC II ICP-MS (USA), as described by Lu et al. (2020). The instrument was equipped with nickel sampler and skimmer cones, and internal standard (0.19 μM rhodium) was added to each sample. The plasma used in the ICP-MS analysis was 99.999% argon, and the optimized plasma gas flow rate (GFR), nebulizer GFR and auxiliary GFR were 15.0 L, 0.88 and 1.2 L min^{-1}, respectively. All calibration curves were obtained before analysis and each sample was measured in parallel 3 times. The baseline drift caused by instrument operation was eliminated by correcting the curves every 30 samples. The method blanks, parallel samples and spiked samples were sequentially analyzed, and the relative standard deviation (RSD) of parallel samples (n = 3) should < 10% (Wang et al., 2018).

2.3.2 Dissolved organic carbon determination

After pre-processing, saturated mercury chloride ($HgCl_2$) was added to the subsamples and then stored in pre-combusted borosilicate glass bottles (500°C, 5 h) for DOC analysis. Then, they were acidified with concentrated phosphoric acid (H_3PO_4) to pH ≤ 2 to remove all the dissolved inorganic carbon. Finally, all processed samples were analyzed using a total organic carbon analyzer (vario TOC select, Elementar, Germany) (Lu et al., 2021). The calibration curve was obtained before analysis and 3 parallel subsamples were measured for each CFU unit. As quality control, the entire detection system was checked after 7 consecutive sample injections using a reference material according to GSB07-1967-2005 developed by Institute for Environmental Reference Materials of Ministry of Environmental Protection (China), and the coefficient of variation on 5 repeated injections should be guaranteed to < 2% (Yang and Gao, 2019). The colloidal organic carbon (COC) data was obtained from the above-mentioned detection method after the water sample was processed by CFU.

2.4 Contamination factor of heavy metals

The CF was applied for the evaluation of water quality in our recent study (Lu et al., 2021). The corresponding value reflects the pollution level of a single heavy metal and overall trace metals in the matrix.

$$CF = \frac{C_{HM}}{C_{back\ ground}}$$

where $C_{background}$ is the quality standard background value of the corresponding metal in seawater, C_{HM} is total dissolved (TD) concentration of the corresponding metal. Due to the lack of background data on all the Heavy metals studied in YRE, the background concentrations were used the grade-one seawater quality standard issued by Administration of Quality Supervision, Inspection and Quarantine of China instead (i.e., 78.68 nmol L^{-1} Cu, 305.90 nmol L^{-1} Zn, 8.90 nmol L^{-1} Cd, 4.83 nmol L^{-1} Pb; GB 3097-1997) (AQSIQ, 1997). The CFs of seawater standards and the samples were summarized in Table 1.

2.5 Data and figure analysis

In this paper, the sampling site bitmap was drawn using CorelDRAW 12, Surfer, and Ocean Data View software, and the data map was drawn using Origin 2021 software. The statistical analysis of the data was carried out using Microsoft Excel 2010 and SPSS 19.0 software to determine the relationship between the relevant parameters. The statistical methods used in this paper mainly include linear regression and Pearson correlation analysis. Among them, Pearson correlation analysis was mainly used to determine the relationship between various

TABLE 1 The summary of the CF values of the sampling sites and seawater standard. Standard values were interpreted as recommended by Hakanson (1980) and Lü et al. (2015).

	Value				Contaminant level
	Cu	Zn	Cd	Pb	
Grade-one seawater quality standard (AQSIQ, 1997) (nmol L^{-1})	78.68	305.90	8.90	4.83	–
Grade-two seawater quality standard (AQSIQ, 1997) (nmol L^{-1})	157.37	764.76	44.48	24.13	–
Concentrations of YRE/(Average) (nmol L^{-1})	1.75-51.32 (31.54)	71.89-501.60(227.04)	0.89-1.87 (1.32)	0.85-2.29 (1.39)	–
CFs of YRE/(Average)	0.02-0.65(0.41)	0.24-1.64 (0.74)	0.10-0.21 (0.15)	0.18-0.47 (0.29)	–
CF standard	CF < 1	–	–	–	Low
	1 ≤ CF < 3	–	–	–	Moderate
	3 ≤ CF < 6	–	–	–	Considerable
	CF ≥ 6	–	–	–	Very high

environmental parameters involved. In the process of statistical analysis, when $p > 0.05$, the two sets of data were significantly correlated, on the contrary, if $p < 0.05$, the correlation was not significant.

3 Results

3.1 General environmental features

For the spatiotemporal characteristics of salinity, temperature, DO, pH and DOC during the investigations in the study area, their partial information has been previously reported (Lu et al., 2021). Overall, the water pH was relatively stable with the values from 7.52 to 8.41, while the salinity ranged widely from 0.52 to 33.04 (Table S1). It is evident that salinity reduction caused by strong mixing behavior occurred at most stations in autumn, while the mixing decreased from sea to land in spring (Table S1).

The DO values of surface water in the YRE ranged from 5.63 to 17.94 mg L^{-1}, and the temperature ranged from 3.3 to 15.8°C. In autumn, DO values dropped below 8.17 mg L^{-1} (Table S1), while DO concentration was > 15.26 mg L^{-1} in spring. Notably, the relatively lower DO concentration occurred in the mixing zone in autumn, indicating the important influence of mixing behavior on the DO dynamics.

3.2 Spatiotemporal variations in DOC

As for each dissolved fraction of DOC, the <1 kDa, 1-3 kDa, 3-10 kDa, 10-100 kDa and 100 kDa-0.45 μm fraction were 116.80-269.78, 0.04-162.59, 0.29-23.51, 0-30.87 and 3.96-94.03 μmol L^{-1} in spring, respectively, with averages of 200.16, 61.86, 8.45, 11.37 and 23.93 μmol L^{-1}, respectively (Figure 2A). In autumn, the corresponding values of DOC were 106.89-253.75 μmol L^{-1} in the <1 kDa fraction, 0.11-10.15 μmol L^{-11} in the 1-3 kDa fraction, 0.31-40.12 μmol L^{-1} in the 3-10 kDa fraction, 0.03-31.24 μmol L^{-1} in the 10-100 kDa fraction, and 0.39-6.18 μmol L^{-1} in the 100 kDa-0.45 μm fraction (Figure 2B). As for the percentages (Figure 3), truly dissolved DOC (<1 kDa) in spring was 35%-92% of their respective total dissolved pools (<0.45 μm), the 1-3 kDa fraction was 0.01%-49%, the 3-10 kDa fractions was 0.1%-7%, the 10-100 kDa fractions was 0%-9%, and the 100 kDa-0.45 μm fractions was 2%-23%; in autumn, the corresponding values of DOC in the five dissolved fractions were

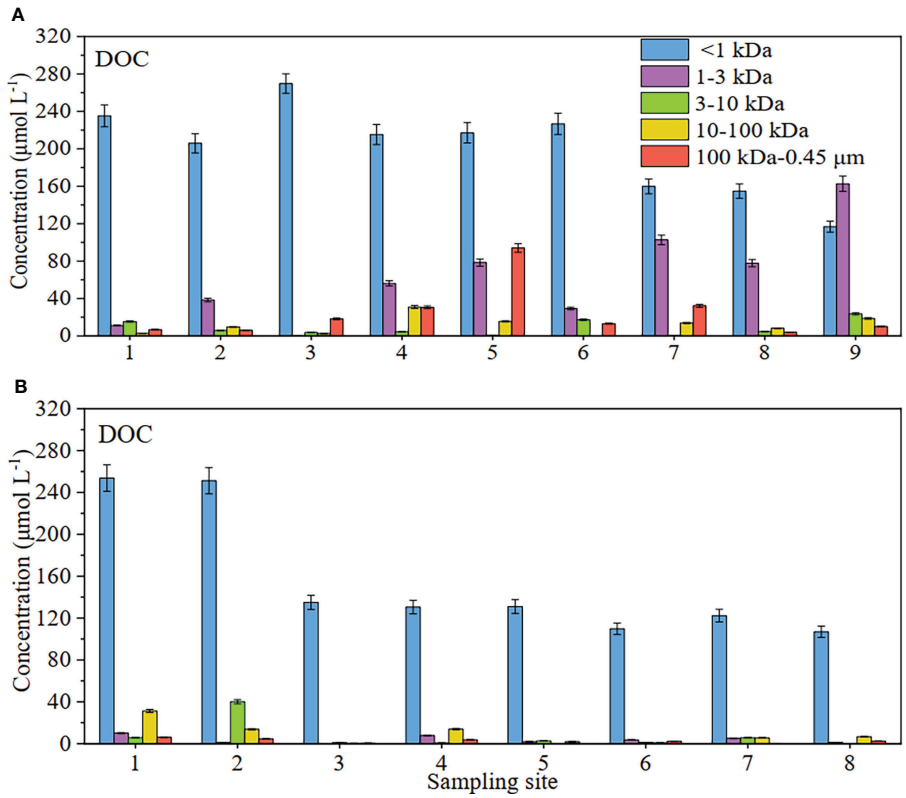

FIGURE 2
Concentration distribution of DOC at different sites in surface waters of the Yellow River Estuary in spring **(A)** and autumn **(B)**.

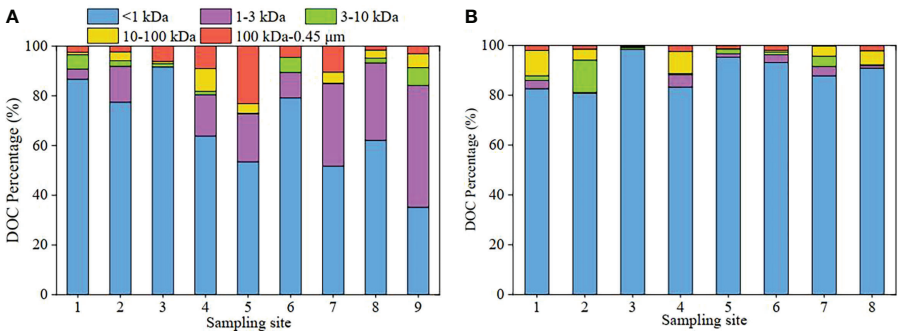

FIGURE 3
Percentage distribution of DOC at different sites in surface waters of the Yellow River Estuary in spring **(A)** and autumn **(B)**.

81%-98%, 0.1%-5%, 0.3%-13%, 0.03%-10% and 0.3%-2%, respectively. Obviously, the high values of DOC fractions were mainly distributed in the <1 kDa of both investigations in the surface water. As for 1 kDa-0.45 μm colloidal DOC, the high DOC values were mainly observed in the 1-3 kDa LMW fraction except for the autumn (Figures 2 and 3). In the autumntime, the colloidal DOC values were significantly lower than those in the <1 kDa fraction of the study area in the surface water, especially HMW (100 kDa-0.45 μm).

3.3 Dissolved metal concentrations

The distribution and CF of the heavy metals (Cu, Zn, Cd and Pb) in the YRE is presented in Figure 4. The concentrations of <0.45 μm TD fraction Fe, Mn, Cu, Zn, Cd and Pb during the two different seasons are presented in Table 2. In spring, six dissolved metal concentrations occurred in the following order: Zn > Fe > Cu > Mn > Cd > Pb. The TD Fe, Mn, Cu, Zn, Cd and Pb concentrations have ranges of 55.85-64.73 (60.17), 33.35-92.40 (46.54), 43.02-51.32 (47.73), 198.84-296.08 (251.03), 1.24-1.87 (1.44) and 0.85-1.43 (1.08) nmol L^{-1}, respectively (Table 2). The highest TD Fe concentration was found at site Y1, followed by that found in sites Y5 and Y4. The spatial pattern of nearshore concentration was higher than that of off shore concentration, reflecting the influence of river input in spring. The highest TD Mn concentration was found at Y1, followed by Y3 and Y6. Higher TD Zn concentrations were found in the eastern parts of the YRE. Similar distribution patterns were found in TD Cd and TD Pb. High concentrations of TD Cu and TD Zn were found in the middle parts of the study area, indicating the addition phenomenon in the middle salinity zone (or mixing zone) (Waeles et al., 2008). As for the autumn, the corresponding metal concentrations occurred in the following order: Zn > Fe > Mn > Cu > Pb > Cd. The concentrations of TD Fe, Mn, Cu, Zn, Cd and Pb ranged from 18.83 to 104.61, 23.18 to 83.30, 1.75 to 29.22, 71.89 to 501.6, 0.89 to 1.59 and 1.15 to 2.29 nmol L^{-1}, respectively, with averages of 62.30, 48.18, 15.35, 203.05, 1.20 and 1.70 nmol L^{-1}, respectively (Table 2). Significantly different from the spring, the highest concentration of TD Fe was found at Y3, followed by that found in Y5 and Y8. Similar distribution patterns were found in TD Mn, TD Cu and TD Zn, suggesting a clear contribution from the Yellow River input. Different from the above four elements, the higher concentrations of TD Pb appeared at Y1 and Y8 and showed dynamic fluctuations in the mixing area, which was similar to the distribution of TD Cd. In summary, the concentrations of TD Fe and Pb are elevated in autumn and have the lower values in spring, and the concentrations of TD Mn, Cu, Zn and Cd are elevated in spring and have the lower values in autumn.

We compared the corresponding results with other aquatic systems (Table 2) and found that the concentrations of TD Fe in the YRE were lower that of the Venice Lagoon (7.69-1124.92 nmol L^{-1}) in Martin and Dai (1995); TD Mn concentrations were higher than that of Venice Lagoon (11.12-44.26 nmol L^{-1}) (Martin and Dai, 1995), but lower than that of Port Jackson (5.95-1838.44 nmol L^{-1}) (Hatje et al., 2003); TD Cu levels were comparable with the similar area in Tang et al. (2010) (1.57-70.19 nmol L^{-1}) but higher than that in Pearl River Estuary (5.35-51.30 nmol L^{-1}) (Zhang et al., 2012), Venice Lagoon (3.15-8.85 nmol L^{-1}) (Martin and Dai, 1995) and Port Jackson (14.64-40.13 nmol L^{-1}) (Hatje et al., 2003); the concentrations of TD Zn, Cd and Pb were lower than that of the study by Tang et al. (2010) in similar area (183.54-1251.76 nmol L^{-1}, 0.89-28.64 nmol L^{-1} and 1.06-48.90 nmol L^{-1}, respectively); due to the application of the clean sampling method and the filter device, the TD Cd and TD Pb concentrations were relatively lower than the study of Wang et al. (2018) in the similar area (0.89-16.90 nmol L^{-1} Cd and 2.02-64.19 nmol L^{-1} Pb), but higher than Venice Lagoon (0.01-0.13 nmol L^{-1} Cd and 0.05-1.08 nmol L^{-1} Pb) and Port Jackson (0.03-0.50 nmol L^{-1} Pb).

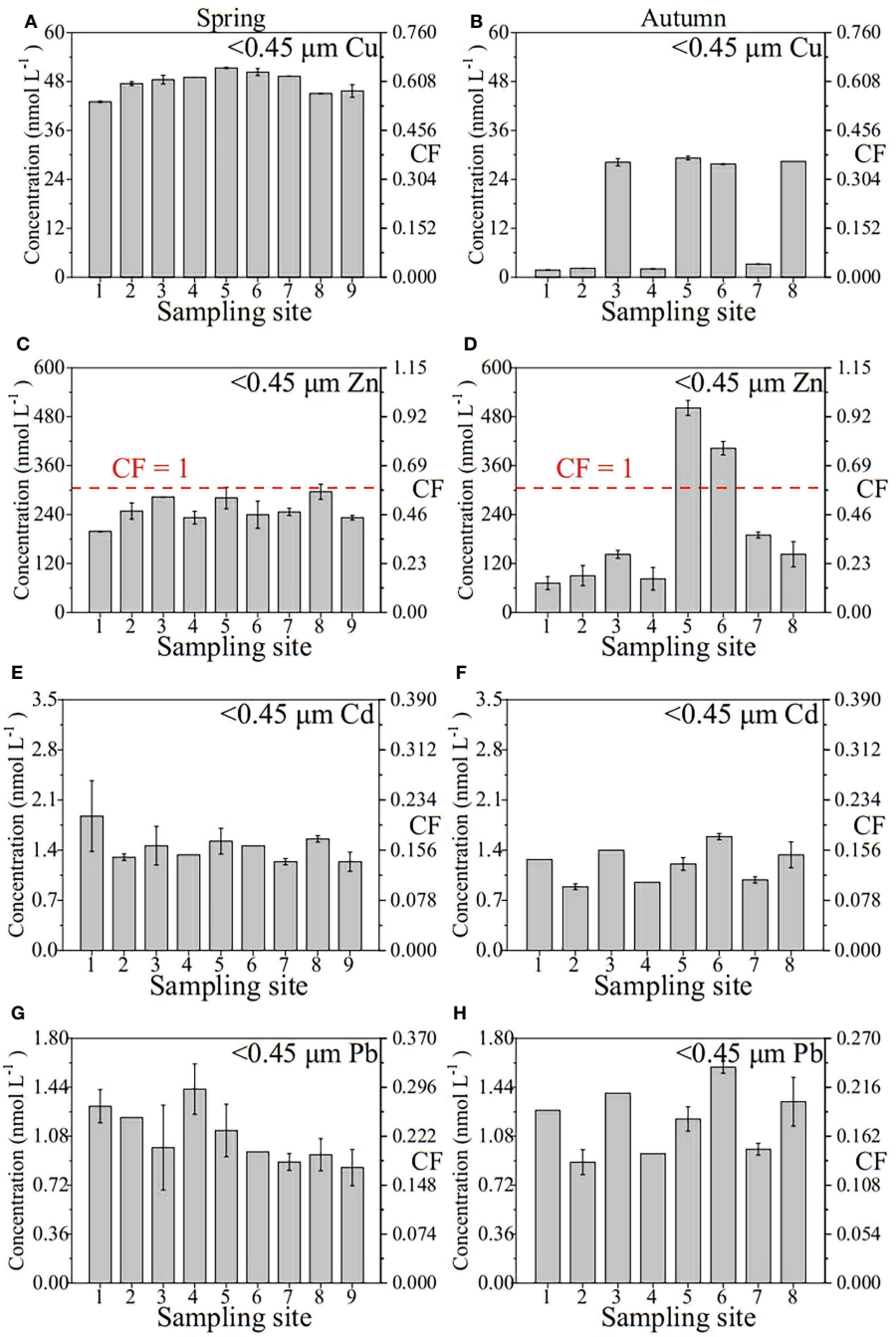

FIGURE 4
Concentration distribution and CF of Cu, Zn, Cd and Pb in the TD phase of the samples of the Yellow River Estuary in spring **(A, C, E** and **G)**; autumn **(B, D, F** and **H)**.

3.4 CF values of Cu, Zn, Cd and Pb

The concentrations of dissolved heavy metals (Cu, Zn, Cd and Pb) in YRE were assessed in accordance to the seawater quality standards of China (Table 1). The contamination levels were assessed according to the CF value standards (Table 1). The concentrations of TD Cu, Cd, and Pb at each site of the two voyages in spring and autumn were lower than the GB 3097-1997 (the grade-one standard), and the CFs ranged from 0.02-0.65 of Cu (average ~0.41), 0.10-0.21 of Cd (~0.15) and 0.18-0.47 of Pb (~0.29), respectively, which indicated low contaminant

TABLE 2 The summary of Fe, Mn, Cu, Zn, Cd and Pb) concentrations in the water of the Yellow River Estuary (YRE) and other estuarine systems in the world (nmol L^{-1}).

Region	Sample		Fe data	Mn data	Cu data	Zn data	Cd data	Pb data	Reference
YRE, China (spring)	Estuarine water	Range/ Mean	55.85-64.73 (60.17)	33.35-92.40 (46.54)	43.02-51.32 (47.73)	198.84-296.08 (251.03)	1.24-1.87 (1.44)	0.85-1.43 (1.08)	This study
YRE, China (autumn)	Estuarine water	Range/ Mean	18.83-104.61 (62.30)	23.18-80.30 (46.18)	1.75-29.22 (15.35)	71.89-501.60 (203.05)	0.89-1.59 (1.20)	1.15-2.29 (1.70)	This study
YRE, China	Estuarine water	Range/ Mean	- [a]	–	1.57-70.19 (41.70)	183.54-1251.76 (576.63)	0.89-28.64 (6.05)	1.06-48.90 (2.46)	Tang et al. (2010)
YRE, China	Estuarine water	Range/ Mean	–	–	0.63-487.84 (182.54)	30.13-645.46 (227.90)	0.89-16.90 (5.87)	2.02-64.19 (27.08)	Wang et al. (2018)
Pearl River Estuary, China	Estuarine water	Range/ Mean	–	–	5.35-51.30 (25.81)	207.10	0.01-2.67 (1.07)	0.92-22.10 (7.77)	Zhang et al. (2012)
Venice Lagoon, Italy	Coastal water	Range	7.69-1124.92	11.12-44.26	3.15-8.85	–	0.01-0.13	0.05-1.08	Martin and Dai (1995)
Port Jackson, Australia	Estuarine water	Range	–	5.95–1838.44	14.64-40.13	50.02-147.75	–	0.03-0.50	Hatje et al. (2003)

[a]"-" represents no relevant reference data.

level. For TD Zn, the CF value of site 5 and 6 in autumn exceeded moderate contaminant levels, while the CFs of the remaining sites were all < 1. In spring, the CF values of all sites showed low pollution levels. In fact, using the grade-one seawater quality standard as contamination background may rank the results differently, so realistic contamination levels may be higher than in our study.

3.5 Dissolved metals in various molecular weight fractions

The concentration and percentage results of the dissolved Fe, Mn, Cu, Zn, Cd and Pb for each fraction are shown in Figures 5 and Figure 6, respectively. A comparison of concentrations and percentages of each dissolved metal in Yellow River samples and other aquatic systems is shown in Table 3.

3.5.1 Concentration distribution

The results showed that the <1 kDa fraction of Fe, Mn, Cu, Zn, Cd and Pb in spring (Figures 5A, C, E, G, I and K) were 38.41-59.14, 23.34-76.13, 23.35-31.81, 140.15-200.73, 0.86-1.24 and 0.05-0.45 nmol L^{-1}, respectively, the 1-3 kDa fraction were 0.08-2.51, 0-2.76, 0.01-4.24, 1.97-55.02, 0-0.19 and 0-0.14 nmol L^{-1}, respectively, the 3-10 kDa fraction were 0.05-3.23, 0-1.77, 0.08-1.16, 0.76-63.48, 0-0.16 and 0-0.19 nmol L^{-1}, respectively, the 10-100 kDa fraction were 0.04-4.60, 0.05-3.27, 0.01-2.80, 0.40-83.12, 0-0.16 and 0-0.51 nmol L^{-1}, respectively, and the 100 kDa-0.45 µm fraction were 0.55-15.63, 7.49-14.99, 12.06-22.57, 4.23-84.61, 0.03-0.60 and 0.06-1.24 nmol L^{-1}, respectively. In autumn (Figures 5B, D, F, H, J and L5), the concentrations of Fe, Mn, Cu, Zn, Cd and Pb were 18.56-94.98 13.44-63.71, 0.77-15.32, 68.75-384.71, 0.64-1.24 and 0.66-1.51 nmol L^{-1} in the <1 kDa fraction, 0.04-5.72, 0.54-7.08, 0.03-2.64, 0.28-29.83, 0-0.22 and 0.03-0.32 nmol L^{-1} in the 1-3 kDa fraction, 0.03-4.45, 0-7.87, 0-2.09, 0.28-26.89, 0-0.22 and 0-0.50 nmol L^{-1} in the 3-10 kDa fraction, 0.04-0.80, 0-2.78, 0.03-1.52, 0.60-19.80, 0-0.13 and 0-0.23 nmol L^{-1} in the 10-100 kDa fraction, and 0.04-3.52, 0.43-53.27,0.87-14.46, 0.40-189.14, 0-0.38 and 0.03-1.01 nmol L^{-1} in the 100 kDa-0.45 µm fraction.

3.5.2 Percentage distribution

As for the percentages (Figure 6), truly dissolved Fe, Mn, Cu, Zn, Cd and Pb in spring (<1 kDa) in spring were 68%-97%, 59%-82%, 46%-65%, 47%-86%, 54%-95% and 5%-37% of their respective <0.45 µm total dissolved pools, respectively, the 1-3 kDa fraction were 0.1%-4%, 0%-7%, 0.01%-10%, 1%-24%, 0%-13% and 0%-14%, respectively, the 3-10 kDa fractions were 0.1%-5%, 0%-2%, 0.2%-2%, 0.3%-22%, 0%-8% and 0%-15%, respectively, the 10-100 kDa fractions were 0.1%-7%, 0.2%-9%, 0.03%-5%, 0.2%-30%, 0%-13% and 0%-60%, respectively, and the 100 kDa-0.45 µm fractions were 1%-27%, 14%-38%, 28%-45%, 2%-29%, 2%-37% and 8%-87%, respectively. In autumn, the corresponding values of Fe in the five fractions were 70%-99%, 0.2%-12%, 0.1%-10%, 0.2%-2% and 0.2%-9%, respectively, the percentages of Mn in the Five fractions were 17%-86%, 1%-31%, 0%-12%, 0%-4% and 1%-66%, respectively, the percentages of Cu were 31%-54%, 0.2%-9%, 0%-7%, 0.2%-5% and 46%-51%, respectively, the percentages of Zn were 42%-97%, 0.1%-6%, 0.4%-9%, 1%-16% and 1%-56%, respectively, the percentages of Cd were 65%-89%, 0%-23%, 0%-18%, 0%-13% and 0%-30%, respectively, and the percentages of Pb were 44%-84%, 2%-18%, 0%-32%, 0%-10% and 2%-46%, respectively.

Obviously, for the four colloidal fractions (1-3 kDa, 3-10 kDa, 10-100 kDa and 100 kDa-0.45 µm fraction), six target metals were more likely to bind to the colloid with a molecular

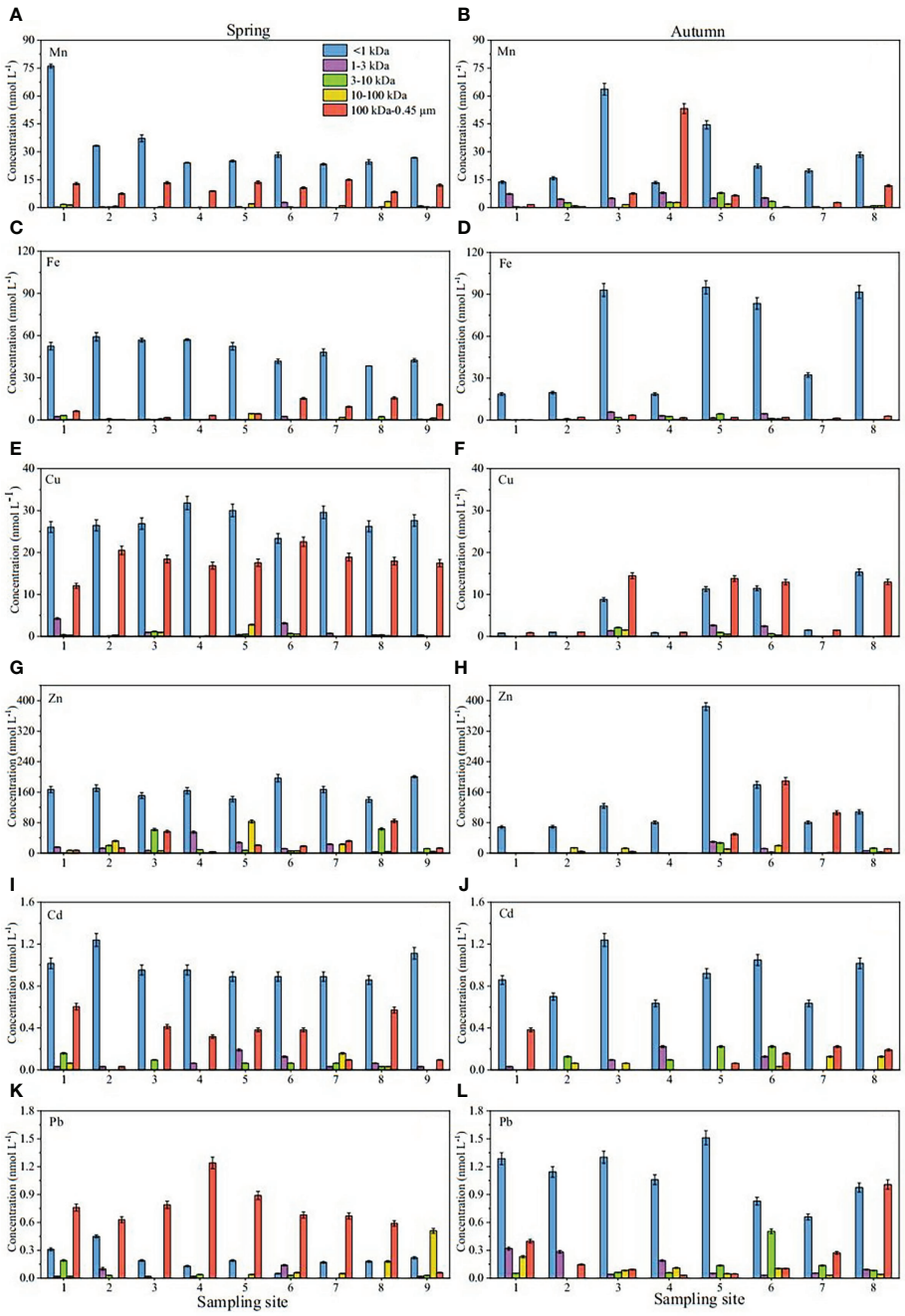

FIGURE 5
Concentration distribution of Mn, Fe, Cu, Zn, Cd and Pb at different sites in surface waters of the Yellow River Estuary in spring **(A, C, E, G, I** and **K)**; autumn **(B, D, F, H, J** and **L)**.

weight of 100 kDa-0.45 μm in spring, indicating that the colloidal matter of this size range may play a significant role in its biogeochemical cycle in this season, which is similar to the previous report data by Wen et al. (1999). In autumn, the difference was that Fe was more inclined to combine with small molecular colloids (1-3 and 3-10 kDa), while other metals were still dominated by HMW (100 kDa-0.45 μm) colloids. In general, the proportion of colloidal metals in their respective total dissolved pools was significantly higher in spring than in autumn.

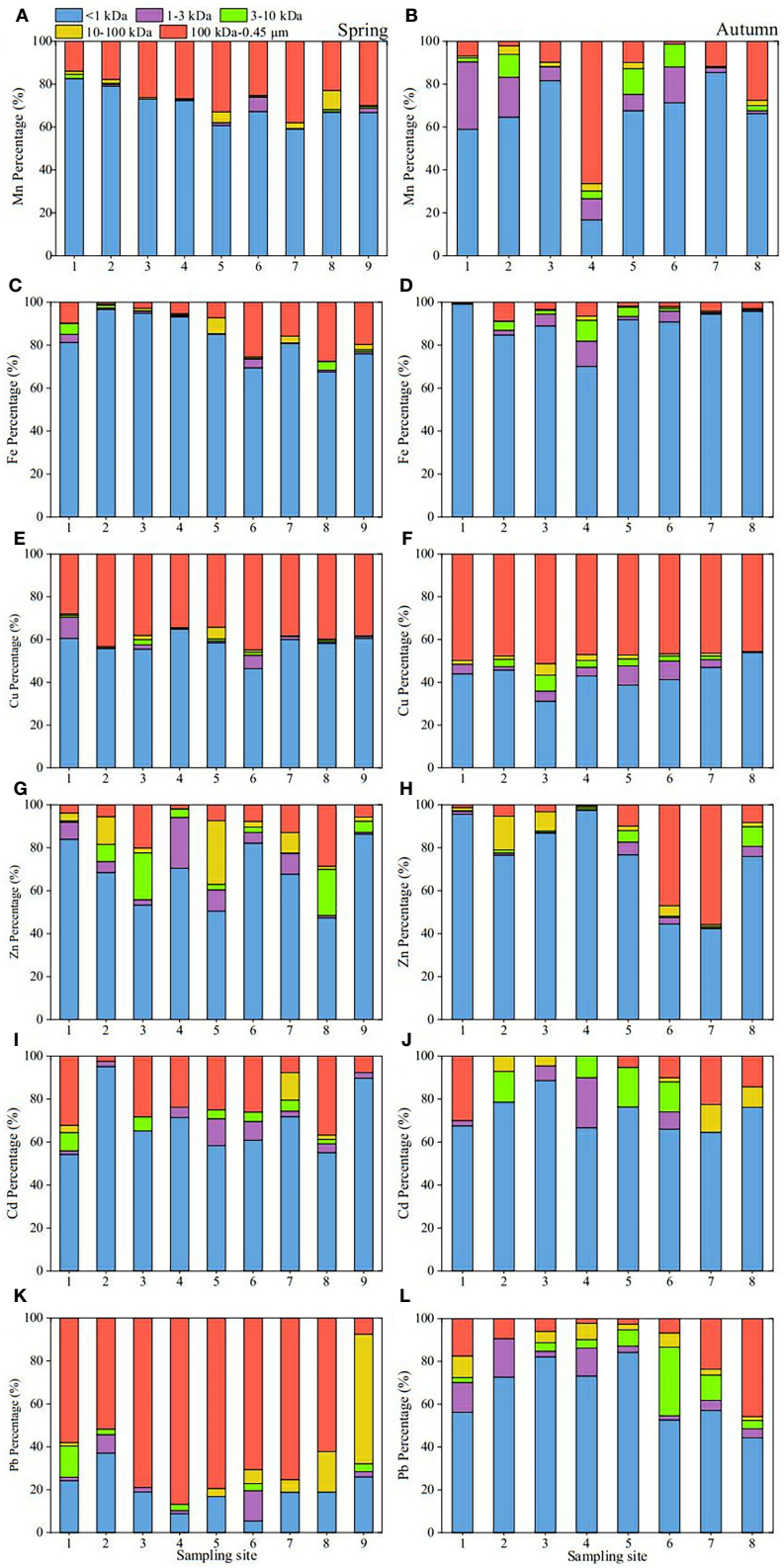

FIGURE 6
Percentage distribution of Mn, Fe, Cu, Zn, Cd and Pb at different sites in surface waters of the Yellow River Estuary in spring **(A, C, E, G, I** and **K)**; autumn **(B, D, F, H, J** and **L)**.

TABLE 3 A comparison of the colloidal metal data in this study and the other literature. C_C and $C_T$represent the concentrations of the colloidal phase and TD phase, respectively.

Region	C_C (nmol L^{-1})						C_C/C_T (%)						Reference
	Fe	Mn	Cu	Zn	Cd	Pb	Fe	Mn	Cu	Zn	Cd	Pb	
YRE, China	0.16-18.47	3.37-66.86	0.98-26.97	2.17-223.43	0.06-0.86	0.28-1.30	1-32	15-83	35-69	3-58	5-46	16-95	This study
Venice Lagoon, Italy	5.21-1121.67	4.50-26.42	1.18-8.34	- [a]	0.001-0.04	0.002-0.98	68-100	24-77	21-59	–	1-63	3-95	Martin and Dai (1995)
Lake Taihu, China	62.72-444.09	5.64-29.49	7.24-13.53	31.51-126.03	0.06-0.16	12.64-17.86	32-81	16-75	13-32	7-54	38-86	11-27	Lu et al. 2020, Lu et al. 2021
Penzé estuary, France	–	–	2.14-2.86	–	0.07-0.30	0.03-0.27	–	–	93-95	–	82	91	Waeles et al. (2008)
North Yellow Sea, China	–	–	5.35 and 5.19	–	0.04 and 0.10	2.75 and 8.20	–	–	31 and 51	–	47 and 50	31 and 50	Lu et al. (2019)
Urban riverine and estuarine waters, China	–	–	0.24-6.88	–	0.02-0.05	0.23-1.11	–	–	17-24	–	10-20	10-42	Lu et al. (2020)

[a]"-" represents no relevant reference data.

4 Discussion

4.1 Effect of salinity on the metal dynamics

Changes in the concentration of chloride irons may significantly affect the behaviors of many trace metals in the aquatic environment (Colombo et al., 2008; Sanders et al., 2015). This phenomenon has been found in many previous studies, which is particularly obvious in the river-sea continuum (or estuary area) (Byrne and Yao, 2000). In this study, limited significant correlations were found in spring for six metals, with only colloid Pb with >10 kDa size fraction showing significant relationships with salinity (Figure 7). Among them, 10-100 kDa was negatively correlated with salinity ($P < 0.05$), while 100 kDa -0.45 µm showed a significant positive correlation ($P < 0.05$), indicating that colloidal Pb tended to form a stable HMW state in this season (Lu et al., 2020). In autumn, however, intriguing correlations between salinity and metal dynamics were discovered. For each dissolved fraction, <1 kDa truly dissolved Fe, Mn, Cu and Cd concentrations positively correlated with salinity, and the 1-3 kDa Pb concentrations negatively correlated with the salinity (P < 0.05) (Figure 7). The positive relations between each corresponding concentration suggest that they may have a common origin (Duan et al., 2010), while the negative correlation may be attributed to the coagulation/flocculation of LMW colloids to the HMW forms (Lu et al., 2021). It is noteworthy that TD Fe, Cu and Cd all showed significant positive correlations with salinity, and there was no significant correlation for TD Mn, Zn and Pb. The data reported by Sanders et al. (2015) in the Korogoro Creek of New South Wales (Australia) proved that the behavior of TD Fe in the estuary with a wide range of salinity (5-35) conformed to the characteristic of gradually decreasing with increasing salinity,

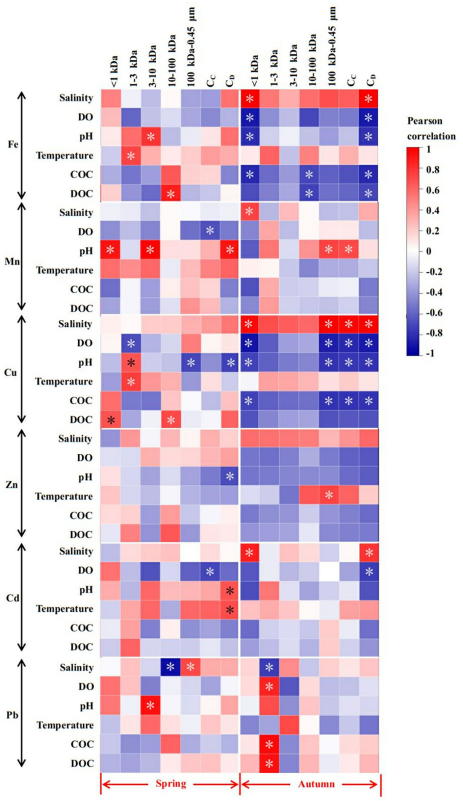

FIGURE 7
Pearson correlation matrix for the concentrations of dissolved Mn, Fe, Cu, Zn, Cd and Pb and the physicochemical parameters in different seasons of YRE. * represents significant (P < 0.05).

but results herein indicate that the dominant total dissolved Fe, Cu and Cd in the mixing zone may not be input from the river but the organic colloid addition on the particle surface, which is similar to the report by Waeles et al. (2008) in the France riverine water. For other colloidal fractions, only 100 kDa-0.45 μm Cu and the whole colloidal Cu were significantly positively correlated with salinity. Since the medium salinity region (salinity 20-30) of the estuarine area often has the phenomenon of metal desorption from the surface of the particulate matter into the water body, although Lu et al. (2020) investigation in the river water of Yantai City (China) found that this situation was more likely to occur in winter, but obviously, this behavior may not be ignored in autumn.

4.2 Effect of DO, pH and temperature on the metal dynamics

Studies have shown that factors such as DO, pH and temperature may affect the migration of elements in the particulate matter-organic matter mixed system (Lu et al., 2021). In addition, Fe, Mn, Cu, and Zn have long been thought to be closely related to phytoplankton growth (Huang et al., 2014; Han et al., 2021), while colloids Cd and Pb have been shown to possess seasonal variation characteristics (Lu et al., 2020; Lu et al., 2022). However, DO, an important biological indicator, did not show a significant correlation with each dissolved fraction of Fe, Zn and Pb in spring (Figure 7). As for other metals, only 1-3 kDa Cu was significantly negatively correlated with DO. Generally, <10 kDa colloids in the aquatic system were primarily considered to be fresh peptides or humic/fulvic compounds (Lu et al., 2020). However, 1 kDa-0.45μm Mn and Cd were significantly negatively correlated with DO, and the increase of DO concentration easily promoted the growth of phytoplankton and further promoted the formation of organic colloid ligands (Lu et al., 2021). Therefore, the behavior of colloid Mn and Cd in spring may be related to the behavior of inorganic colloidal ligands. For pH and temperature, a similar situation occurred for <10 kDa Fe, Mn, Cu and Pb, that is, there were significant positive correlations with pH, which proved the higher activity of colloid of this size fraction. Different from spring, HMW colloids in autumn, especially >10 kDa Mn and Zn, were significantly related to the dynamic changes of DO, pH and temperature. In addition, the truly dissolved Fe, Cu and other <1 kDa biotrophic metal elements showed high activity (Figure 7). Compared to spring (March), the increase of temperature in autumn (November) may promote the growth of plankton in the water, and the released substances such as peptidoglycans, proteins and extracellular polysaccharides may promote the overall increase of HMW organic ligand concentrations, which may be an important factor in increasing the HMW colloidal trace metal percentages (Kaplan et al., 1987; Lee et al., 1996; Hung et al., 2001; Lead and Wilkinson, 2006). However, the significant downward trend of the relationship between 1-100 kDa fraction and environmental parameters (except Pb) proves that the flocculation or coagulation of LMW colloids in autumn was considerable. Generally, LMW organics in aquatic environments were considered to be newly released polypeptides or humus/fulvic compounds (Lu et al., 2020).

4.3 Effect of COC/DOC on the metal dynamics

DOC, as an important component in dissolved organic matter (DOM), is a key carbon source for the growth and metabolism of planktonic bacteria, and its bioavailability has always been the focus and hotspot of ecosystem research (Li et al., 2008). In addition, DOC is an important indicator to explore the relationship between elemental behavior and organic matter (Lu et al., 2021). In spring, only the concentrations of 10-100 kDa fraction colloidal Fe and Cu were closely related to the DOC concentration ($p < 0.05$) (Figure 7), suggesting that they may have a common organic origin (Duan et al., 2010; Lu et al., 2021). On the contrary, the result in autumn indicated that negative relations of 10-100 kDa Fe vs. COC and DOC ($p < 0.05$) and 100 kDa-0.45 μm and 1 kDa-0.45 μm Cu vs. COC ($p < 0.05$), which suggested that the main source of HMW colloidal Fe and Cu in this season may be the inorganic sources rather than organic matter or the decomposition of organic ligands on the surface of particles (Mavrocordatos et al., 2000; Stolpe et al., 2013). However, 1-3 kDa Pb showed significant positive correlation with COC and DOC ($p < 0.05$), indicating that Pb behavior was still mainly affected by organic ligands in this season. These intriguing phenomena may prove the heterogeneity of colloids in the YRE. First, the concentration of DOC in the TRE is much lower than the average level of DOC in the world's rivers of ~416.67 μmol L^{-1} (0.5 mg L^{-1}) (Meybeck, 1982; Lu et al., 2021). Also, the lower light transmittance brought by the turbid water body limits the effective growth of phytoplankton to a certain extent (Pakulski et al., 2000). The combined effect of the above two may lead to an insignificant relationship between the colloidal metal and the organic ligands in the YRE. Secondly, the disturbance of sediment caused by strong hydrodynamics and the river-sea mixing behavior make the trace elements, particulate matter and organic matter may undergo violent migration and transformation in a limited area (Skrabal et al., 1997; Sun et al., 2007; Santos-Echeandia et al., 2008; Janot et al., 2012; Bao et al., 2019). Dai and Martin (1995) and Dai et al. (1995) assumed that the colloidal matter consisted of at least two parts: one part was stable in physicochemical properties (ie: the conserved part) and the other part was removed at the river-sea interface. Among them, unlike proteins containing multiple amino acid residues and humic acid (as a mixture), carbohydrates usually possess stable

structures. Among them, many studies have shown that the behavior of carbohydrates, an important carbon source, may significantly affect the behavior of colloidal metals in aquatic environments (Xu et al., 2018a). In addition, carbohydrate tends to form a colloidal system with network structures in saline systems, which could result in a stable behavior of the colloidal phase after flocculation (Guo et al., 2009). Obviously, in the YRE mixing area, the non-conservative part may dominate the geochemical behavior of colloidal metals in the spring and autumn. However, the contribution of inorganic colloidal ligands should not be ignored.

4.4 Effect of organic matter-particle mixture system on the metal dynamics

However, a single influencing factor is difficult to exist. In other words in the natural aquatic environment, the migration of dissolved metal may be affected by the organic matter-particle mixture system. First, the organic matter and particulate matter compete with the free metals in the water environment (Wood, 1996; Sures and Zimmermann, 2007), and then causing the metals to migrate between the organic (or colloidal) and particulate phases, mainly determined by the physical and chemical properties of particulate matter and organic matter. Secondly, trace elements can inhibit their adsorption on the particulate matter when they are considered to be stable complexes with small organic ligands and inorganic ligands in water systems (Zakharova, 1987; Wood, 1996; Cobelo-García, 2013; Liu et al., 2019). In addition, the presence of organic matter in the water may change the surface properties of the particles, and the adhesion of different organic matter to the surface of different particles may cause the surface area and potential of the particles to change together, which may directly affect the migration of the elements between the two (Liu and Gao, 2019). Hence, more comprehensive demonstration of the metal migration process in complex aquatic systems may not be allowed to proceed based on limited data. However, the results obtained can still provide some insights into the heterogeneity of colloidal metals in the aquatic environment of this region.

5 Conclusions

Over this study, clean sampling technology and modified CFU method have proved their high efficiency to separate and determine the various dissolved fractions of Fe, Mn, Cu, Zn, Cd and Pb in the YRE. All the CF values were <1 except TD Zn at station 5 and 6 in autumn (CF = 1.64 and 1.32), indicating lower contaminant levels of the YRE. Our results have shown that the concentration and percentage of 100 kDa-0.45 μm HMW metals were dominant in the YRE drainage system except for 1-10 kDa Fe in autumn. The size-fractionation variations of six colloidal metals along the environmental parameters were examined and some insights affecting the migration of the dissolved fraction from the river to seawater in this system were provided: (a) the TD Fe, Mn, Cu, Zn, Cd and Pb concentration exhibits non-conservative behavior from the river to sea; (b) the addition of colloidal metals in the middle salinity region should be attributed to the contribution of the colloidal ligand, especially colloidal Fe, Cu and Cd; (c) strong ligand, mixing process and desorption from the surface of the particles co-regulate colloidal metals of the YRE; (d) the distributions of Fe, Cu and Pb are affected by the characteristics of DOC or COC to a certain extent, but this is limited to the >10 kDa HMW colloidal Pb and <10 kDa LMW colloidal Fe and Cu. However, whether the lower and stable DOC level in the YRE region has a stronger effect on colloidal metals than suspended particles or sediments remains to be further studied. In addition, the quantitative effect of phytoplankton on dissolved metals or each dissolved fraction should also be studied further. In summary, although the factors affecting the migration of colloidal metals are comprehensive and complex, the results obtained in this paper may still enrich the existing knowledge of colloids and biogeochemical cycling for better understanding of the dynamic behaviors of trace metals in aquatic systems.

Data availability statement

The datasets presented in this study can be found in online repositories. The names of the repository/repositories and accession number(s) can be found in the article/Supplementary Material.

Author contributions

FL and TY: Investigation, formal analysis, conceptualization, methodology, validation, writing - original draft. YL and NW: Funding acquisition, resources, conceptualization, methodology, validation, supervision, writing - review & editing. All authors contributed to the article and approved the submitted version.

Funding

This work was financially supported by the National Natural Science Foundation of China (No. 42207520 and 51903247), the Natural Science Foundation of Shandong Province (ZR2022QD127) and the Fundamental Research Projects of Science & Technology Innovation and Development Plan in Yantai City (No. 2022MSGY063). The assistance of Prof. Dawei Pan in voyage and the sample collection is greatly appreciated.

Conflict of interest

The authors declare that the research was conducted in the absence of any commercial or financial relationships that could be construed as a potential conflict of interest.

Publisher's note

All claims expressed in this article are solely those of the authors and do not necessarily represent those of their affiliated organizations, or those of the publisher, the editors and the reviewers. Any product that may be evaluated in this article, or claim that may be made by its manufacturer, is not guaranteed or endorsed by the publisher.

Supplementary material

The Supplementary Material for this article can be found online at: https://www.frontiersin.org/articles/10.3389/fmars.2022.1074829/full#supplementary-material

References

AQSIQ (1997). "Sea Water quality standard (GB 3097-1997)," in *Administration of quality supervision, inspection and quarantine* (Beijing: Standard Press of China).

Bao, T. L., Wang, P. F., Hu, B., and Shi, Y. (2019). Investigation on the effects of sediment resuspension on the binding of colloidal organic matter to copper using fluorescence techniques. *Chemosphere* 236, 124312. doi: 10.1016/j.chemosphere.2019.07.043

Bi, N. S., Yang, Z. S., Wang, H. J., Xu, C. L., and Guo, Z. G. (2014). Impact of artificial water and sediment discharge regulation in the huanghe (Yellow river) on the transport of particulate heavy metals to the sea. *Catena* 121, 232–240. doi: 10.1016/j.catena.2014.05.006

Byrne, R. H., and Yao, W. S. (2000). Formation of palladium(II) hydroxychloride complexes and precipitates in sodium chloride solutions and seawater. *Geochim. Cosmochim. Ac.* 64, 4153–4156. doi: 10.1016/S0016-7037(00)00501-9

Cobelo-García, A. (2013). Kinetic effects on the interactions of Rh(III) with humic acids as determined using size-exclusion chromatography (SEC). *Environ. Sci. pollut. Res.* 20 (4), 2330–2339. doi: 10.1007/s11356-012-1113-8

Colombo, C., Oates, C. J., Monhemius, A. J., and Plant, J. A. (2008). Complexation of platinum, palladium and rhodium with inorganic ligands in the environment. *Geochem.-Explor. Env. A.* 8, 91–101. doi: 10.1144/1467-7873/07-151

Cornu, S., Samouëlian, A., Ayzac, A., and Montagne, D. (2018). Soluble and colloidal translocation of Al, fe, Si and Mn in an artificially drained French retisol. *Geoderma* 330, 193–203. doi: 10.1016/j.geoderma.2018.05.032

Dai, M. H., and Martin, J. M. (1995). First data on trace metal level and behaviour in two major Arctic river-estuarine systems (Ob and yenisey) and in the adjacent kara Sea, Russia. *Earth. Planet. Sc. Lett.* 131, 127–141. doi: 10.1016/0012-821X(95)00021-4

Dai, M. H., Martin, J. M., and Cauwet, G. (1995). The significant role of colloids in the transport and transformation of organic carbon and associated trace metals (Cd, Cu and Ni) in the Rhone delta (France). *Mar. Chem.* 51, 159–175. doi: 10.1016/0012-821X(95)00021-4

Duan, L. Q., Song, J. M., Li, X. G., Yuan, H. M., and Xu, S. S. (2010). Distribution of selenium and its relationship to the eco-environment in bohai bay seawater. *Mar. Chem.* 121, 87–99. doi: 10.1016/j.marchem.2010.03.007

González-Álvarez, R. J., Bellido-Millab, D., Pinto, J. J., and Moreno, C. (2020). A handling-free methodology for rapid determination of Cu species in seawater based on direct solid micro-samplers analysis by high-resolution continuum source graphite furnace atomic absorption spectrometry. *Talanta* 206, 120249. doi: 10.1016/j.talanta.2019.120249

Guo, L. D., and Santschi, P. H. (2007). "Ultrafiltration and its applications to sampling and characterisation of aquatic colloids," in *Environmental colloids and particles: Behavior, separation and characterisation*. Eds. K. Wilkinson and J. Lead (Chichester: John Wiley & Sons Ltd.), 159–221.

Guo, L., Sun, C. M., Li, G. Y., Liu, C. P., and Ji, C. N. (2009). Thermodynamics and kinetics of Zn(II) adsorption on crosslinked starch phosphates. *J. Hazard. Mater.* 161 (1), 510–515. doi: 10.3724/SP.J.1095.2014.40065

Hakanson, L. (1980). An ecological risk index for aquatic pollution control. A sedimentological approach. *Water Res.* 14, 975–1001. doi: 10.1016/0043-1354(80)90143-8

Han, H. T., Pan, D. W., Pan, F., Hu, X. P., and Zhu, R. L. (2021). A functional micro-needle sensor for voltammetric determination of iron in coastal waters. *Sensor. Actuat. B-Chem.* 327, 128883. doi: 10.1016/j.snb.2020.128883

Hatje, V., Apte, S. C., Hales, L. T., and Birch, G. F. (2003). Dissolved trace metal distributions in port Jackson estuary (Sydney harbour). *Aust. Mar. pollut. Bull.* 46, 719–730. doi: 10.1016/j.csr.2013.11.014

Huang, P., Li, T. G., Li, A. C., Yu, X. K., and Hu, N. J. (2014). Distribution, enrichment and sources of heavy metals in surface sediments of the north yellow Sea. *Cont. Shelf Res.* 73, 1–13. doi: 10.1016/j.csr.2013.11.014. Yu.

Hung, C. C., Tang, D., Warnken, K. W., and Santschi, P. H. (2001). Distributions of carbohydrates, including uronic acids, in estuarine waters of Galveston bay. *Mar. Chem.* 73 (3-4), 305–318. doi: 10.1016/S0304-4203(00)00114-6

Illuminati, S., Annibaldi, A., Romagnoli, T., Libani, G., Antonucci, M., Scarponi, G., et al. (2017). Distribution of cd, Pb and Cu between dissolved fraction, inorganic particulate and phytoplankton in seawater of Terra Nova bay (Ross Sea, Antarctica) during austral summer 2011-12. *Chemosphere* 185, 1122–1135. doi: 10.1016/j.chemosphere.2017.07.087

Janot, N., Reiller, P. E., Zheng, X., Croue, J. P., and Benedetti, M. F. (2012). Characterization of humic acid reactivity modifications due to adsorption onto a-Al_2O_3. *Water Res.* 46 (3), 731–740. doi: 10.1016/j.watres.2011.11.042

Kaplan, D., Christiaen, D., and Arad (Malis), S. (1987). Chelating properties of extracellular polysaccharides from chlorella spp. *Appl. Environ. Microb.* 53, 2953–2956. doi: 10.1128/aem.53.12.2953-2956.1987

Lead, J. R., and Wilkinson, K. J. (2006). Natural aquatic colloids: current knowledge and future trends. *Environ. Chem.* 3, 159–171. doi: 10.1071/EN06025

Lee, J. G., Ahner, B. A., and Morel, F. M. M. (1996). Export of cadmium and phytochelatin by the marine diatom thalassiosira weissflogii. *Environ. Sci. Technol.* 30, 1814–1821. doi: 10.1021/es950331p

Liang, Y., Pan, D. W., Wang, C. C., Lu, Y. X., and Fan, X. (2022). Distribution and ecological health risk assessment of dissolved trace metals in surface and bottom seawater of yantai offshore, China. *Front. Mar. Sci.* 9. doi: 10.3389/fmars.2022.993965

Lin, H. Y., Sun, T., Xue, S. F., and Jiang, X. L. (2016). Heavy metal spatial variation, bioaccumulation, and risk assessment of *Zostera japonica* habitat in the YRE, China. *Sci. Total Environ.* 541, 435–443. doi: 10.1016/j.scitotenv.2015.09.050

Liu, K., and Gao, X. L. (2019). Adsorption and fractionation of pt, pd and Rh onto inorganic microparticles and the effects of macromolecular organic compounds in seawater. *Environ. pollut.* 255, 113192. doi: 10.1016/j.envpol.2019.113192

Liu, K., Gao, X. L., Li, L., Chen, C. T. A., and Xing, Q. G. (2018). Determination of ultra-trace pt, pd and Rh in seawater using an offline pre-concentration method and inductively coupled plasma mass spectrometry. *Chemosphere* 212, 429–437. doi: 10.1016/j.chemosphere.2018.08.098

Liu, K., Gao, X. L., Xing, Q. G., and Chen, F. S. (2019). Adsorption kinetics of platinum group elements onto macromolecular organic matter in seawater. *Acta Oceanol. Sin.* 38 (8), 8–16. doi: 10.1007/s13131-019-1433-3

Liu, R. X., Lead, J. R., and Zhang, H. (2013). Combining cross flow ultrafiltration and diffusion gradients in thin-films approaches to determine trace metal speciation in freshwaters. *Geochim. Cosmochim. Ac.* 109, 14–26. doi: 10.1016/j.gca.2013.01.030

Liu, H. Q., Liu, G. J., Wang, J., Yang, Z. J., and Da, C. N. (2016a). Fractional distribution and risk assessment of heavy metals in sediments collected from the yellow river, China. *Environ. Sci. pollut. Res.* 23, 11076–11084. doi: 10.1007/s11356-016-6291-3

Liu, H. Q., Liu, G. J., Wang, S. S., Zhou, C. C., Yuan, Z. J., and Da, C. N. (2016b). Distribution of heavy metals, stable isotope ratios (^{d}13C and ^{d}15N) and risk assessment of fish from the YRE, China. *Chemosphere* 208, 731–739. doi: 10.1016/j.chemosphere.2018.06.028

Li, W., Wu, F. C., Liu, C. Q., Fu, P. Q., Wang, J., Mei, Y., et al. (2008). Temporal and spatial distributions of dissolved organic carbon and nitrogen in two small lakes on the southwestern China plateau. *Limnology* 9 (2), 163–171. doi: 10.1007/s10201-008-0241-9

Lu, Y. X., Gao, X. L., and Chen, C. T. A. (2019). Separation and determination of colloidal trace metals in seawater by cross-flow ultrafiltration, liquid-liquid extraction and ICP-MS. *Mar. Chem.* 215, 103685. doi: 10.1016/j.marchem.2019.103685

Lu, Y. X., Gao, X. L., Song, J. M., Chen, C. T. A., and Chu, J. L. (2020). Colloidal toxic trace metals in urban riverine and estuarine waters of yantai city, southern coast of north yellow Sea. *Sci. Total Environ.* 717, 135265. doi: 10.1016/j.scitotenv.2019.135265

Lu, Y. X., Pan, D. W., Yang, T. T., and Wang, C. C. (2021). Spatial and environmental characteristics of colloidal trace Cu in the surface water of the yellow river estuary, China. *Mar. pollut. Bull.* 168, 112401. doi: 10.1016/j.marpolbul.2021.112401

Lu, Y. X., Pan, D. W., Yang, T. T., and Wang, C. C. (2022). Distribution characteristics and controlling factors of typical heavy metals in yellow river estuary of China. *J. Oceanol. Limnol.* doi: 10.1007/s00343-021-1320-6

Lü, D., Zheng, B., Fang, Y., Shen, G., and Liu, H. J. (2015). Distribution and pollution assessment of trace metals in seawater and sediment in Laizhou Bay. *China. J. Oceanol. Limnol.* 33, 1053–61. doi: 10.1007/s00343-015-4226-3

Martin, J. M., and Dai, M. H. (1995). Significance of colloids in the biogeochemical cycling of organic carbon and trace metals in the Venice lagoon (Italy). *Limnol. Oceanogr.* 40 (1), 119–131. doi: 10.4319/lo.1995.40.1.0119

Mavrocordatos, D., Mondi-Couture, C., Atteia, O., Leppard, G. G., and Perret, D. (2000). Formation of a distinct class of fe-Ca(-C_{org})-rich particles in a complex peat-karst system. *J. Hydrol.* 237, 234–247. doi: 10.1016/S0022-1694(00)00309-7

Meybeck, M. (1982). Carbon, nitrogen and phosphorus transport by world rivers. *Am. J. Sci.* 282, 401–450. doi: 10.1016/j.crte.2004.09.016

Milliman, J. D., and Ren, M.-E. (1995). *Climate change: Impact on coastal habitation*. Ed. E. Eisma (Boca Raton, Florida: CRC Press), 57–83.

Pakulski, J., Benner, R., Whitledge, T., Amon, R., Eadie, B., Cifuentes, L., et al. (2000). Microbial metabolism and nutrient cycling in the Mississippi and atchafalaya river plumes. *Estuar. Coast. Shelf Sci.* 50 (2), 173–184. doi: 10.1006/ecss.1999.0561

Peers, G., and Price, N. M. (2006). Copper-containing plastocyanin used for electron transport by an oceanic diatom. *Nature* 441(7091), 341–344. doi: 10.1038/nature04630

Qiao, S. Q., Yang, Z. S., Pan, Y. J., and Guo, Z. G. (2007). Metals in suspended sediments from the changjiang (Yangtze river) and huanghe (Yellow river) to the sea, and their comparison. *Estuar. Coast. Shelf Sci.* 74, 539–548. doi: 10.1016/j.ecss.2007.05.042

Sanders, C. J., Santos, I. R., Maher, D. T., Sadat-Noori, M., Schnetger, B., and Brumsack, H. (2015). Dissolved iron exports from an estuary surrounded by coastal wetlands: Can small estuaries be a significant source of fe to the ocean? *Mar. Chem.* 176, 75–82. doi: 10.1016/j.marchem.2015.07.009

Santos-Echeandia, J., Laglera, L. M., Prego, R., and van den Berg, C. M. G. (2008). Dissolved copper speciation behavior during estuarine mixing in the San Simon inlet (wet season, galicia). influence of perticulate matter. *Estuar. Coast. Shelf S.* 76, 447–453. doi: 10.1016/j.ecss.2007.07.007

Skrabal, S. A., Donat, J. R., and Burdige, D. J. (1997). Fluxes of copper-complexing ligands from estuarine sediments. *Limnol. Oceanogr.* 42, 992–996. doi: 10.2307/2838904

Statham, P. J., Jacobson, Y., and van den Berg, C. M. G. (2012). The measurement of organically complexed Fe^{II} in natural waters using competitive ligand reverse titration. *Anal. Chim. Acta* 743, 111–116. doi: 10.1016/j.aca.2012.07.014

Stolpe, B., Guo, L. D., Shiller, A. M., and Aiken, G. R. (2013). Abundance, size distributions and trace-element binding of organic and iron-rich nanocolloids in alaskan rivers, as revealed by field-flow fractionation and ICP-MS. *Geochim. Cosmochim. Ac.* 105, 221–239. doi: 10.1016/j.gca.2012.11.018

Sun, X. J., Qin, B. Q., Zhu, G. W., and Zhang, Z. P. (2007). Effect of wind-induced wave on concentration of colloidal nutrient and phytoplankton in lake taihu. *Environ. Sci.* 28 (3), 506–511. doi: 10.13227/j.hjkx.2007.03.011

Sures, B., and Zimmermann, S. (2007). Impact of humic substances on the aqueous solubility, uptake and bioaccumulation of platinum, palladium and rhodium in exposure studies with dreissena polymorpha. *Environ. pollut.* 146 (2), 444–451. doi: 10.1016/j.envpol.2006.07.004

Tang, A., Liu, R., Ling, M., Xu, L., and Wang, J. (2010). Distribution characteristics and controlling factors of soluble heavy metals in the YRE and adjacent sea. *Proc. Environ. Sci.* 2, 1193–1198. doi: 10.1016/j.proenv.2010.10.129

Waeles, M., Tanguy, V., Lespes, G., and Riso, R. D. (2008). Behavior of colloidal trace metals (Cu, Pb and cd) in estuarine waters: An approach using frontal ultrafiltration (UF) and stripping chronopotentiometric methods (SCP). *Estuar. Coast. Shelf S.* 80, 538–544. doi: 10.1016/j.ecss.2008.09.010

Wang, Y., Liu, R. H., Zhang, Y. Q., Cui, X. Q., Tang, A. K., and Zhang, L. J. (2016). Transport of heavy metals in the huanghe river estuary, China. *Environ. Earth Sci.* 75, 288. doi: 10.1007/s12665-015-4908-3

Wang, C., Wang, W., He, S., Du, J., and Sun, Z. (2011). Sources and distribution of aliphatic and polycyclic aromatic hydrocarbons in yellow river delta nature reserve, China. *Appl. Geochem.* 26, 1330–1336. doi: 10.1016/j.apgeochem.2011.05.006

Wang, X. Y., Zhao, L. L., Xu, H. Z., and Zhang, X. M. (2018). Spatial and seasonal characteristics of dissolved heavy metals in the surface seawater of the YRE, China. *Mar. pollut. Bull.* 137, 465–473. doi: 10.1016/j.marpolbul.2018.10.052

Wen, L. S., Santschi, P. H., Gill, G., and Paternostro, C. (1999). Estuarine trace metal distributions in Galveston bay: Importance of colloidal forms in the speciation of the dissolved phase. *Mar. Chem.* 63, 185–212. doi: 10.1016/S0304-4203(98)00062-0

Wen, L. S., Santschi, P. H., Warnken, K. W., Davison, W., Zhang, H., Li, H. P., et al. (2011). Molecular weight and chemical reactivity of dissolved trace metals (Cd, Cu, Ni) in surface waters from the Mississippi river to gulf of Mexico. *Estuar. Coast. Shelf S.* 92, 649–658. doi: 10.1016/j.ecss.2011.03.009

Wood, S. A. (1996). The role of humic substances in the transport and fixation of metals of economic interest (Au, pt, pd, U, V). *Ore Geol. Rev.* 11 (95), 1–31. doi: 10.1016/0169-1368(95)00013-5

Xu, H. C., Houghton, E. M., Houghton, C. J., and Guo, L. D. (2018a). Variations in size and composition of colloidal organic matter in a negative freshwater estuary. *Sci. Total Environ.* 615, 931–941. doi: 10.1016/j.scitotenv.2017.10.019

Xu, H. C., Lin, H., Jiang, H. L., and Guo, L. D. (2018b). Dynamic molecular size transformation of aquatic colloidal organic matter as a function of pH and cations. *Water Res.* 144, 543–552. doi: 10.1016/j.watres.2018.07.075

Xu, H. C., Xu, M. W., Li, Y. N., Liu, X., Guo, L. D., and Jiang, H. L. (2018c). Characterization, origin and aggregation behavior of colloids in eutrophic shallow lake. *Water Res.* 142, 176–186. doi: 10.1016/j.watres.2018.05.059

Yang, B., and Gao, X. L. (2019). Chromophoric dissolved organic matter in summer in a coastal mariculture region of northern Shandong peninsula, north yellow Sea. *Cont. Shelf Res.* 176, 19–35. doi: 10.1016/j.csr.2019.02.006

Yang, B., Gao, X. L., Zhao, J. M., Lu, Y. X., and Gao, T. C. (2020). Biogeochemistry of dissolved inorganic nutrients in an oligotrophic coastal mariculture region of the northern Shandong peninsula, north yellow Sea. *Mar. pollut. Bull.* 150, 110693. doi: 10.1016/j.marpolbul.2019.110693

Zakharova, I. A. (1987). Coordination compounds of Pd(II) and Pt(II) with thiodiacetic acid. *Polyhedron* 6 (5), 1065–1070. doi: 10.1016/S0277-5387(00)80956-0

Zhang, J., and Huang, W. W. (1993). Dissolved trace metals in the huanghe: the most turbid large river in the world. *Water Res.* 27 (1), 1–8. doi: 10.1016/0043-1354(93)90188-N

Zhang, D., Zhang, X., Tian, L., Ye, F., Huang, X., Zeng, Y., et al. (2012). Seasonal and spatial dynamics of trace elements in water and sediment from pearl river estuary, south China. *Environ. Earth Sci.* 68, 1053–1063. doi: 10.1007/s12665-012-1807-8

Zhou, Z. Z., Stolpe, B., Guo, L. D., and Shiller, A. M. (2016). Colloidal size spectra, composition and estuarine mixing behavior of DOM in river and estuarine waters of the northern gulf of Mexico. *Geochim. Cosmochim. Ac.* 181, 1–17. doi: 10.1016/j.gca.2016.02.032